Universidad Nacional de Ingeniería

Grupo de estudios aeroespaciales (GEA)

KunturSat

Author 1	Luis Aiquipa M.
Author 2	Katherine Roman M.
Author 3	Marco Rodriguez A.
Author 4	Felixjesus Ramirez T.
Author 5	Juan Villanueva O.
Author 6	Alexander Trigoso S.

first of October 2024

Índice

1. About us

1.1. BIOMET-GEA

We are students from the Universidad Nacional de Ingeniería, located in Lima, Peru. With the growing interest in aerospace and space sciences, the GEA group was founded in 2022 by students from the BIOMET research group within our university Fig.1. To date, our work has focused on control theory, mechanical and electronic design, and simulations.

As a group, our goal is to innovate and promote space sciences through our participation in various international competitions, such as C'space, and in the publication of scientific articles.

Figura 1: photographs of Biomet members.

At Biomet, we are not only focused on the aerospace field, but we also have expertise in instrumentation, bioinorganic chemistry, and ecotoxicology. We have been working in these areas for over 5 years, forming a multidisciplinary group that includes students from Physics Engineering, Electrical Engineering, Mechanical Engineering, and Chemistry.

1.2. Team Organization and Roles

The group is composed of 6 members from the National University of Engineering, as shown in the following organizational chart. See Figure2.

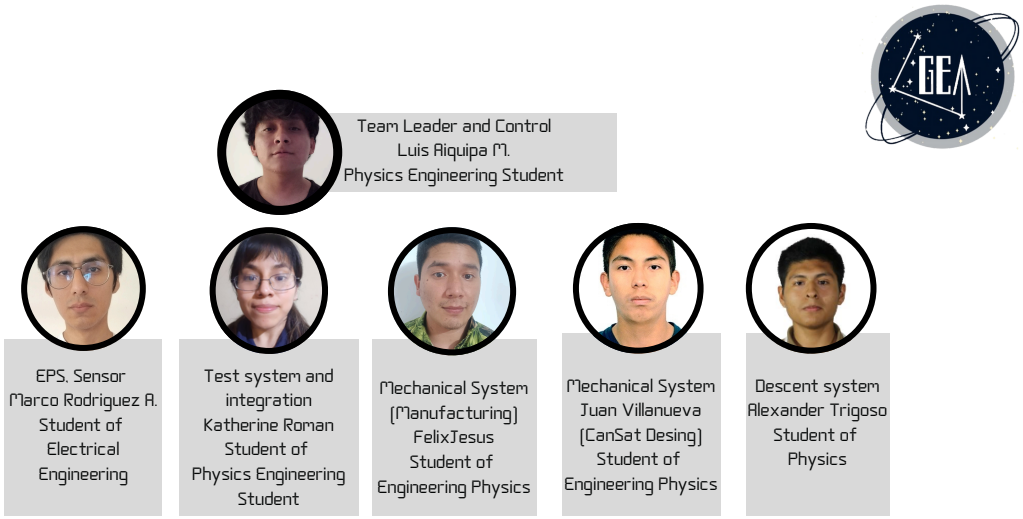

Figura 2: Organigrama del equipo GEA

2. Payload Description

2.1. Missions

Within all the missions designated by the CanSat France 2024 competition , the project selected the main mission and two secondary missions. The main mission involved acquiring the largest possible area on the ground by marking it with a biodegradable liquid or object that is environmentally responsible. Multiple areas can be acquired, and they will be added together. The largest area is at the center of the target point; the farther from the center, the smaller the areas. The target GPS position is 43°13'18.7"N 0°03'10.0"W. The landing zone will be marked with a wooden square, and the marked area will be measured 5 minutes after landing.

The first secondary mission focused on completing the operation in a vertical position, remaining upright for at least 3 minutes, considering the nature of the ground. Finally, the second selected secondary mission was to deploy a flag at least 5 cm by 8 cm, ensuring it does not touch the CanSat once deployed.

2.2. Mechanical Structure

The CanSat resembles a cylindrical structure, which reduces air resistance and distributes stresses more evenly compared to other structures. It consists of several independent parts, whose total assembly has the shape of a cylinder with a height of 200 mm and a diameter of 80 mm. For its design, all parts were modeled using the software *Autodesk® Inventor® 2024*. Figure 4 shows the complete mechanical configuration of the CanSat, with the flagpole oriented downwards, the vertical arms and supports undeployed (Figure 4a), while Figure 4b shows the flag, paraglider and supports deployed. Additionally, Figure 3 provides a detailed view of the mechanisms, including their locations within the assembly and the design features that enable their functionality.

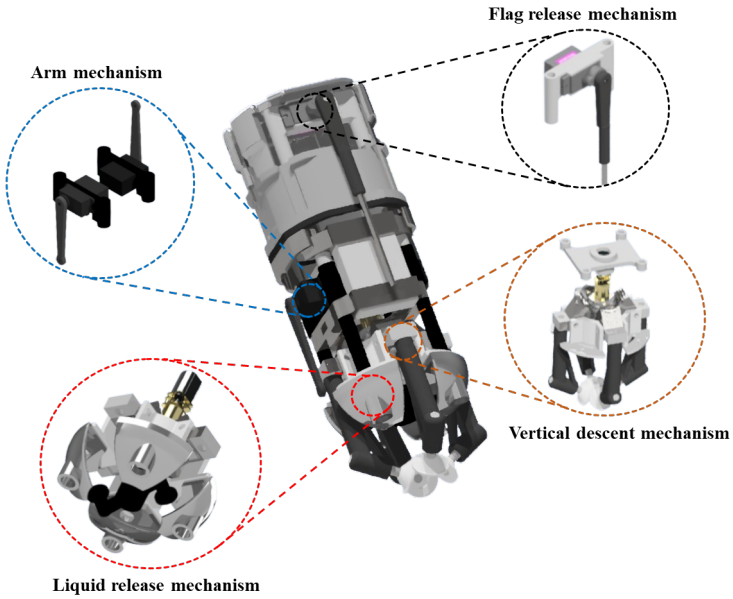

Figura 3: CanSat mechanisms.

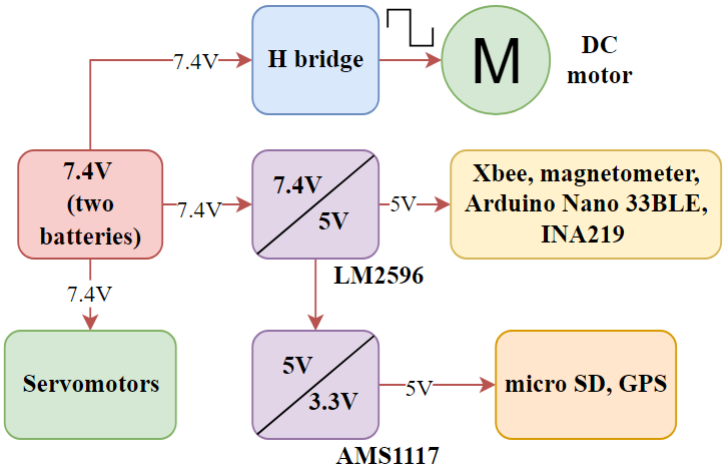

Figura 5: Voltage regulation in the Cansat system

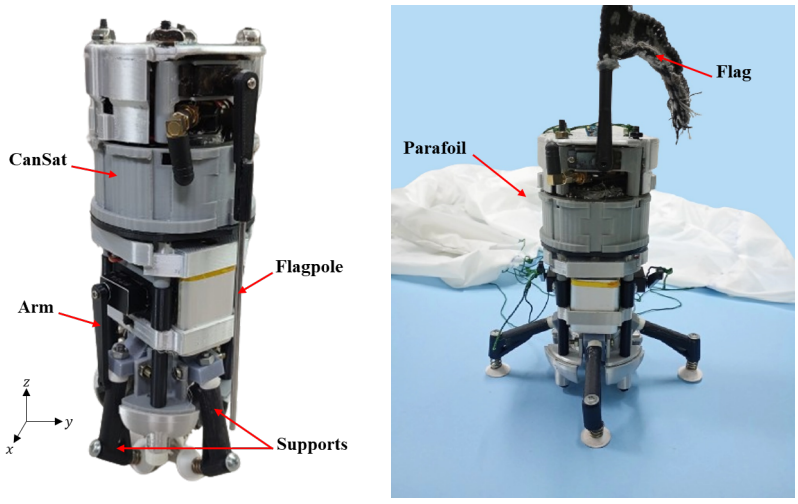

(a) (b)

Figura 4: Complete configuration of the mechanisms in the final assembly.

2.3. Electrical Desing

The power supply system consists of two 3.7 V batteries, which provide a net voltage of 7.4 V to the system. Each battery has 2000 mAh. The batteries are chosen based on the average current consumption of the entire system, mainly for the servomotors and the DC motor, which also determine the maximum consumptions. The Cansat demands a minimum current of 225 mA, an average current of 340 mA and a maximum of 3 A. Determining the amount of maximum or minimum current mostly involves the servomotors and the DC motor showing both their maximum operating power consumption at stall and also their idle power consumption, respectively.

2.3.1. DC-DC regulators

The regulators provide a safe and reliable power supply to the sensors and other devices of the satellite peak. AMS1117 and LM2596 regulators are established for voltage regulation at 3.3 and 5 V respectively for power supply of electronic devices. Figure 5 shows how voltages are regulated in the system. Battery recharging Battery recharging is done with a 3-pin charging connector. Figure 6 shows the schematic connection diagram. Deactivation of the main power supply is necessary for battery charging, and charging does not take place simultaneously.

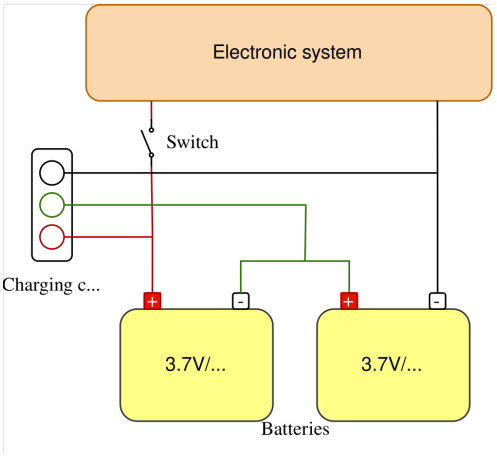

Figura 6: Wiring diagram for battery charging

Cuadro 1: List of system sensors

Sensor N°	Sensor	Brief description	Remarks
1	HTS221	Temperature sensor integrated to the Arduino board with a measuring range from 15 to 40° C with an accuracy of 0.5° C.	It measures temperature in real time as the system descends.
2	LPS22HB	Absolute pressure sensor integrated to the Arduino board with a measuring range from 260 to 1260 hPa.	It measures the pressure at which the value of the satellite peak height is obtained, by means of a linear relationship.
3	LSM9DS1	Sensor integrated to the Arduino board with 3 acceleration channels, 3 angular velocity channels, 3 magnetic field channels.	With this sensor it is possible to determine dynamic magnitudes of the device such as: velocity, acceleration and magnetic field, in the 3 axes (X, Y and Z).
4	INA219	DC current sensor with a range of 0 to 3.2 A with an accuracy of 0.8 mA.	Determine the current consumed by the entire system.
5	HMC5883L	3-axis magnetometer.	Determines the orientation of the Cansat with respect to the Earth's magnetic field to orient the device.

2.4. Electronic system

The electronics of the system consists of an Arduino Nano 33 BLE development board, sensors, a GPS module, a radio frequency module, a motor controller (H-bridge) and three servomotors, the power supply of these peripherals is carried out mainly by 2 batteries of 3.7 V with a charge of 2000 mAh each; these batteries are connected under a series connection, so it gives an input voltage to the system of 7.4 V with 2000 mAh. The direct power supply to the peripherals is provided by regulators that provide voltages of 5 and 3.3 V as required. According to, the Arduino Nano presents versatility and practicality in use, in addition to the suitability of its size and weight for the application in Cansat. The Arduino Nano 33 BLE model presents, in the same way, good characteristics in size and weight, besides containing temperature, pressure and IMU (inertial measurement unit) sensors integrated to the board, which allows in the design of the electronic board of the Cansat system to have smaller dimensions.

2.5. Sensor Subsystem

The sensor subsystem is responsible for taking data: ambient temperature, pressure, tilt angles, current measurement and earth magnetic field. Some of these reside inside the development board. Table 1 shows a list of the different sensors used during the event.

2.6. Parafoil Desing

When the CanSat is released, the only forces acting on it are the force of gravity and the drag force of the wind, which will depend on the shape and size of the glider. The paraglider is the evolution of a steerable parachute that takes greater advantage of dynamic, thermodynamic or thermal updrafts in its displacement (Lopez, 2019). This is the main reason to use it in the project, since it must travel a desired trajectory in order to fulfill the missions requested by the organization.

To calculate the projected area we must take into account the minimum terminal velocity requested by the organization, which was 5m/s. The terminal velocity depends on certain parameters such as: projected area, glider shape, friction coefficient, air density, gravity, mass of the load and wind speed.

With these values in mind, the projected area is calculated using the terminal velocity formula:

$$V_\infty = \sqrt{\frac{2mg}{\rho A C_d}} \tag{1}$$

V_∞: velocidad terminal
m: masa
g: gravedad de la tierra
ρ: densidad del aire
A: Área transversal del parapente
C_d: Coeficiente de arrastre

Taking into account that the air density is $1,204 kg/m^3$, the drag coefficient of the paraglider is 0.7 (Ruiz, 2006), the gravity is $9,81 m/s^2$, the mass used for the calculation is 800g and for a terminal velocity of $5 m/s$ we obtain as a result that the projected area needed for this case the paraglider will be $0.434 m^2$, this value is multiplied by a safety factor of 1.5, with which we obtain the projected area with which the glider will be designed, $0.66 m^2$.

Due to the small size of the CanSat device, only a 9-cell glider was chosen to avoid the complexity in its fabrication and the structure of the ropes that are attached to the CanSat body. The manufacture of the paraglider is composed of 3 stages: (i) manufacture of molds from a software called "SingleSkin version 0.3" which using the parameter of projected area and number of cells gives us the final design of the cells and ribs, (ii) We proceed to make the cells and ribs in a fabric of high resistance to tearing, in this case Ripstop Nylon was used, then we proceeded to join them. (iii) Finally, we put the rope system, which is made of braided nylon, which will go from the glider to the CanSat body and its arms. These stages are illustrated in the figure 7

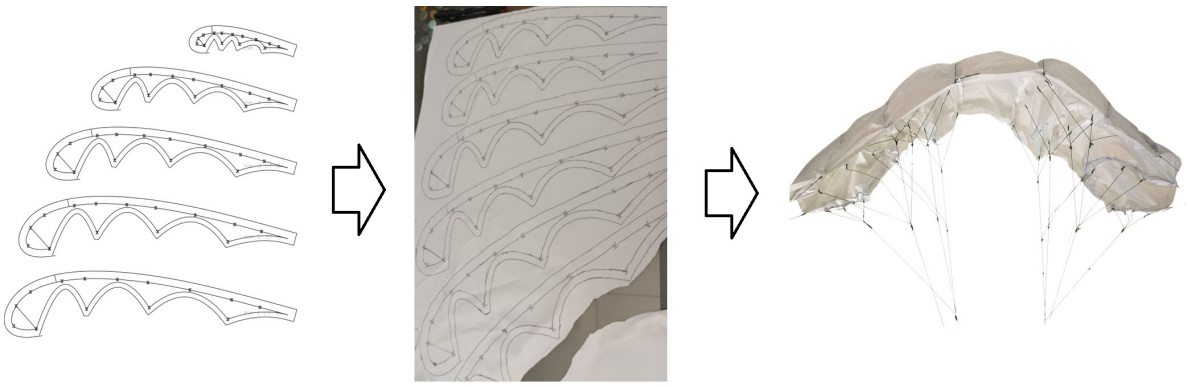

Figura 7: etapas de fabricación del parapente

2.7. liquid release mecanism

As can be seen in the figure 3, there is the ballon braker mechanism, which works together with the worm screw because they share the same shaft that is attached to the DC motor shown in the same figure. The purple chicha balloons go on the internal walls of this system.

Purple chicha was used for this project due to its property of being able to leave stains or leave marks on surfaces, as this contains a natural pigment called cyanidin-3-*beta* glucoside (Manzano, 2016), so purple chicha concentrate was used for May effectiveness.

the system works at the same time as the landing legs are activated. this is how the ballon braker system starts working. The pins at the ends burst the balloons, thus releasing the chicha which serves as a marker.

2.8. Control Desing

A glider with 6 degrees of freedom (DOF) is established, for this purpose a system of inclination arms will be used, these will be responsible for making an angular change with respect to the axis of the device itself, while adapting to changes in wind direction, wind speed and other environmental factors. To achieve these changes in response to environmental disturbances, an autonomous system will be used, which will be composed of a PID controller that will be responsible for precise monitoring of the angle.

2.8.1. PID design process for trayectory tracking

The controller used is necessary to ensure accurate tracking of the yaw angle of orientation. The use of the PID controller unlike other controllers has an ease of implementation, it allows to give a first approximation in the expected results to reduce the errors produced during its work execution, it is also expected that once set the yaw angle to the orientation where the target direction points to release an object of negligible mass, for its analysis it will not be considered the Coriolis effect and neither the drag force since the launch proposes that the height is relatively low.

2.8.2. PID block diagram of Horizontal Trajectory Tracking (HTT) control

Figure 8 shows the block diagram of the controller to follow the horizontal trajectory considering as a model the kinematic equations of rotation and translation given by:

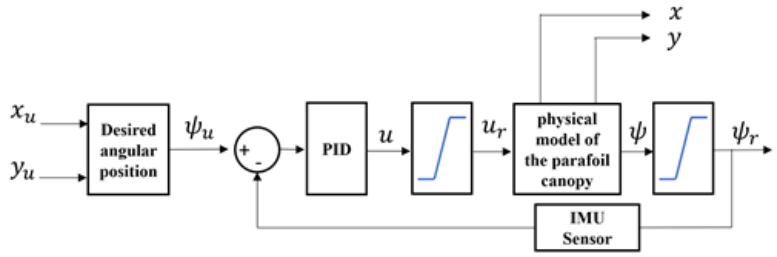

Figura 8: Block diagram of the PID control system of the glider system for trajectory tracking by angular change.

Where ψ_u, the desired orientation angle is given by the desired position inputs (x_u, y_u) following the equation

$$\psi_u = \tan^{-1}\left(\frac{y_u - y_0}{x_u - x_0}\right) \tag{2}$$

The control output u generated by the PID controller must be restricted by saturation to the limit values of the z component of the angular velocity of the canopy parafoil generated by the payload arms. The feedback is given by an inertial measurement sensor to determine the yaw angular change.

2.8.3. HTT simulation results analysis

Ideal considerations were taken to carry out a simulation of this trajectory tracking, such as considering that the mass loss due to the release of the liquid is zero, in addition to ignoring elasticity problems between the ropes, deformation of the glider (this case can occur depending on the wind currents), lift forces of the payload. In addition, the positioning of the liquid release system must be such that it does not affect the center of mass of the payload.

In the simulation, the studied glider model starts at the starting point (0,0,150) m and the target point is (15,12,0) m, In addition to the fact that the descent speed provided by the parachute is 5 m/s, at an altitude of 150 m and the components x and y the angular velocity of the canopy parafoil is 0 $\frac{rad}{s}$. The possible trajectories to reach the target are dependent on the flight plan, it is possible to have two types of trajectory, one helical and one linear. One helical and one linear trajectory is selected for the

mission recapture. The stage starts with a helical trajectory ending at position (2.43,0.516,35.0) m, and then realise the linear trajectory using the PID controller, as shown in Figure 9.

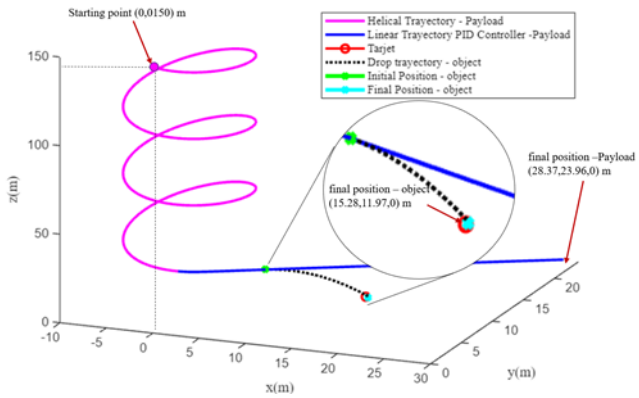

Figura 9: Simulation trajectory plotted for the helical and horizontal trajectory of the payload, as well as the trajectory described for the descent of the object.

The helical trajectory descent is determined by the speed of descent, and the magnitude of the angular variation in the z component of the canopy parafoil. The trajectory is set by the arms and the direction of rotation is dependent on the change of direction, the angular speed considered was 0.838 $\frac{rad}{s}$. At this stage the importance lies in descending without varying much from the initial position since the target is a relatively short distance away.

2.8.4. Arm mechanism

This system uses two 3-pin connectors, which provide both the power and the signal needed to operate the MG90S servomotors. The 2 servomotors are mounted on the sides of the CanSat using their respective supports (Figure 10b), which are made of PC like the flag release mechanism, and have holes for the passage of the rods.

Each SG90 servo motor is equipped with PC-printed arms. These arms, whose design is shown in Figure 10a, are critical to controlling the paraglider. They are attached to the servo motors by a small screw, as they have a small hole at the end. The arms are connected to the paraglider and tension the strings, thus allowing for steering and turning control during flight. Movement of the servo motors adjusts the tension on the strings, resulting in changes in the paraglider's trajectory.

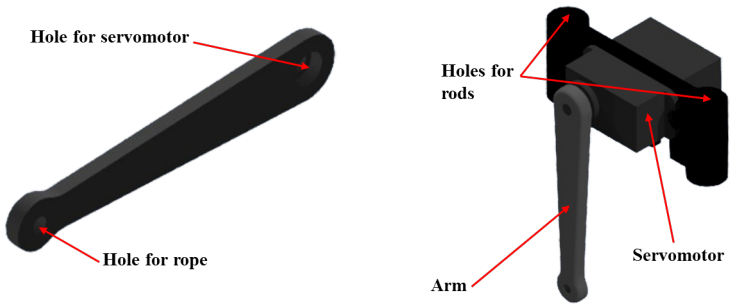

(a) CanSat arm. (b) Servomotor support.

Figura 10: Components of the arm mechanism.

The trajectory control of the arm mechanism is integrated with a GPS module, which is important as it determines the position of the CanSat during its operation. The position information provided by this module is used as a feedback signal for the flight control system, ensuring that the device maintains the desired trajectory and has autonomous control.

3. Results & Discussions

The flight results were obtained at the camp facilities in France, where one primary mission and two secondary missions were carried out: the deployment of a flag and achieving a vertical landing on the ground. Figure 11 illustrates the stages of the flight, from the initial preparation to the landing. KunturSat was placed in a container with a diameter of 95 mm and a height of 300 mm, then activated and its data transmission verified before being released from a drone at 150 meters altitude. During the descent, purple corn drink (*chicha morada*) was released, which triggered the detonation of the internal balloons and the deployment of the supports for vertical descent, while telemetry data was sent to the ground station. Finally, the flag was deployed, marking the end of the descent. The entire flight lasted 46.6 seconds, with a descent speed of 4.55 m/s, and telemetry recorded a landing 400 meters away from the target. The launch test took place around 11:00 AM.

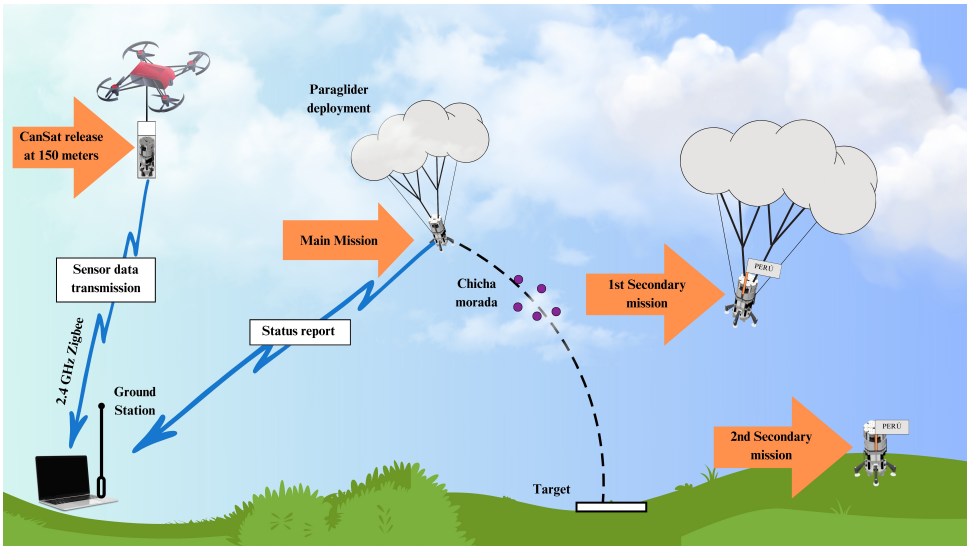

Figura 11: Plan de Vuelo: Etapas de la Misión y Despliegue de Carga Útil

3.1. Misión Principal

Figure 12 shows the evolution of the distance between KunturSat and the target on the ground over time. Initially, a countdown period is observed during the first 10 seconds, followed by the launch of KunturSat at 11.2 seconds. During its descent, the liquid (chicha morada) was released at 40.2 seconds, at which point the system status changed from low to high. After the release, KunturSat continued its trajectory, progressively moving away from the target until reaching a final distance of 125.520 cm, thus concluding its flight.

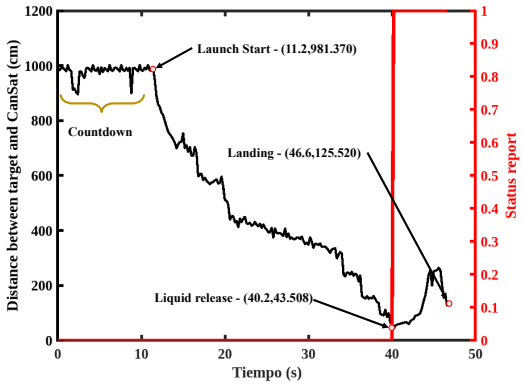

Figura 12: Distancia entre el KunturSat y el objetivo durante la secuencia de aterrizaje

3.2. First Secondary Mission: Flag Deployment

The condition for approaching the target with a 50 cm discrepancy from the programmed target point in the microcontroller was successfully executed, demonstrating the simultaneous operation of both the flag deployment and the support mechanisms during the flight. Figure 13 shows the captured moment where the vertical descent mechanisms and the flag release mechanism perform their functions.

Figura 13: KunturSat Flight Deployment during the C'Space 2024 Event

3.3. Second Secondary Mission: Vertical Positioning

The vertical positioning mission begins with the deployment of the supports, culminating when the system lands on the ground while maintaining its vertical position. Figure 14 shows the angular variation curves during the flight, recorded by the IMU sensor. The final angular variations are 85.11 and 11.52 on the Pitch and Roll axes, respectively. The attached image illustrates the final position of the system after landing.

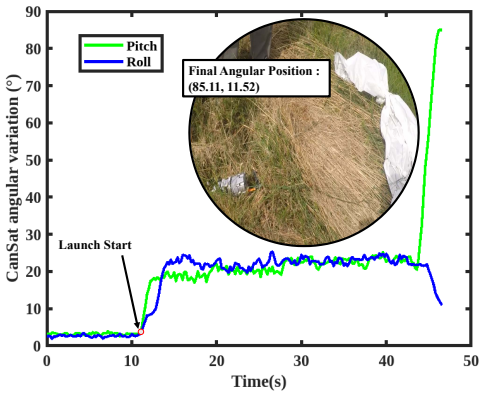

Figura 14: Angular Variation of the CanSat during Flight and Final Position after Landing